Microsystem Technologies 10 (2004) 97–102 © Springer-Verlag 2004
DOI 10.1007/s00542-003-0313-z

Trench filling characteristics of low stress TEOS/ozone oxide deposited by PECVD and SACVD

C. Chang, T. Abe, M. Esashi

Abstract In this paper low stress silicon oxide was deposited with tetraethylorthosilicate (TEOS, $Si(OC_2H_5)_4$)/ozone by plasma enhanced chemical vapor deposition (PECVD) and sub-atmospheric chemical vapor deposition (SACVD) for deep trench filling. Two kinds of PECVD oxide were fabricated: Coil antenna inductively coupled plasma (ICP) oxide and parallel plates capacitive coupled plasma (CCP) oxide. Adding ozone into the deposition process enhances the trench filling capability. Oxide filling in a deep trench (5 μm wide, 52 μm deep) was carried out using the SACVD process, which gave excellent conformal step coverage. However, the coil antenna ICP oxide was suitable as a sealing material. The effects of argon ion sputtering and magnetic field in the PECVD for the trench filling are discussed in this paper. Because the low temperature processes of PECVD and SACVD, the thermal residual stress was reduced and a low stress film of 85 MPa compression is available.

1
Introduction

Recently, in semiconductor application, silicon dioxide serves as insulating dielectrics, and a passivation layer [1]. The SiO_2 layer of vary large-scale integrated (VLSI) devices has to be capable of planarization, trench filling, and reducing parasitic capacitance. Similarly, silicon dioxide is a very attractive MEMS (Microelectromechanical systems) material, because of its low thermal and electrical conductivities, low thermal expansion coefficient, and good mechanical strength. Currently, deep trenches are often encountered both in advanced semiconductors devices (e.g. multilevel interconnections [1]) and in MEMS (e.g. inertial sensing [2]). As MEMS devices continue to further use high aspect ratio processes (e.g. to encapsulate a micromachined device or micro-packaging [3–5]), trench filling greatly simplifies the following technology steps.

The trench-filling layer in MEMS can be a final layer for sealing holes in a membrane over a micromachined device, an etch-stop [6–7], a sacrificial layer (e.g. gyroscope [2]), or a suspended support for thermal isolation (e.g. micromachined heated silicon island [3]) as illustrated in Fig. 1a. For pure planarization or trench filling, conformal step coverage is greatly desired as illustrated in Fig. 1b. Figure 1 shows the trenches discussed in this paper and Fig. 1c shows the trench is partially filled. Here the parameters of the step coverage are defined: the bottom step coverage, b/a, and the sidewall step coverage, c/a [7]. The aspect ratio of a trench is the ratio of the depth to the width of the trench. In many cases a void forms during the film deposition as illustrated in Fig. 1d. However, for sealing a hole in a membrane above a sensitive structure or forming a micro-channel in Power MEMS or Bio MEMS [5, 8], a low bottom step coverage (b/a) and a low sidewall step coverage (c/a) are desired. A thick silicon dioxide layer also provides a variety of application for electrical, thermal isolation, and packaging [3]. In summary, the MEMS requirements for SiO_2 properties are: (1) low residual stress, (2) trench filling capability and surface planarity, (3) low dielectric constant [1, 9]. Especially, the trench filling capability plays important role in MEMS, since the microstructures with high aspect ratios have been rapidly developed.

In this paper plasma enhanced chemical vapor deposition (PECVD) and sub-atmospheric chemical vapor deposition (SACVD) were used to form SiO_2 with the low residual stress, because the depositions were done at low temperature (<400 °C) [10–15]. Most conventional low pressure chemical vapor deposition (LPCVD) processes run at relatively high temperature about 650 °C or higher, resulting in high thermal residual stress. However, LPCVD offers good step coverage and is a strong candidate for filling trenches as well [3–5]. The organic silicon source for PECVD and SACVD, TEOS (tetraethylorthosilicate, or tetraethoxysilane, $Si(OC_2H_5)_4$), and ozone (O_3) provide a superior conformal coverage and trench filling of oxide to those of silane/O_2 due to its movable precursor on the wafer surface [16–18]. In this paper two kinds of PECVD oxide were fabricated: Coil antenna inductively coupled

Received: 5 August 2002 / Accepted: 14 March 2003

C. Chang (✉)
Venture Business Laboratory, Tohoku University,
01 Aza-Aoba, Aramaki, Aoba-ku, Sendai 980-8579, Japan
e-mail: clchang@mems.mech.tohoku.ac.jp

T. Abe
Graduate School of Engineering,
Tohoku University PRESTO, JST,
01 Aza-Aoba, Aramaki, Aoba-ku, Sendai 980-8579, Japan

M. Esashi
New Industry Creation Hatchery Center, Tohoku University,
01 Aza-Aoba, Aramaki, Aoba-ku, Sendai 980-8579, Japan

This work is supported by a Grant-in-Aid (No. 13305010) from Japanese Ministry of Education, Culture, Sports, Science and Technology. A part of this work has been performed in Venture Business Laboratory, Tohoku University.

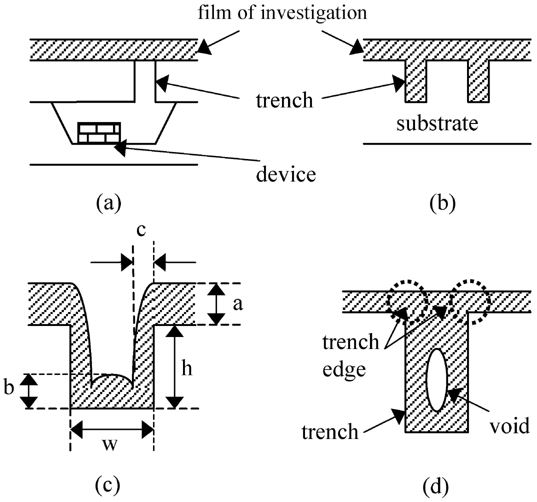

Fig. 1. **a** Sealing over a micromachined device, **b** trench filling and planarization, **c** partially filled trench, **d** a void forms in the trench

plasma (ICP) oxide and parallel plates capacitive coupled plasma (CCP) oxide. Since ICP provides high density plasma (HDP), higher deposition rate can be achieved [19], but poor step coverage and overhang occur. That makes ICP oxide be capable of sealing the trenches. Most important of all, SACVD oxide shows excellent conformal step coverage, and deep trench filling is achieved.

The aim of this paper has been to successfully develop the SACVD TEOS oxide to fill deep trenches, and the ICP oxide to seal the wide trenches. The effects of argon ion sputtering and magnetic field in PECVD processes will be discussed in details. It should be noted that all processes were done in the same chamber, so any kind of PECVD machine can be utilized for this technique of deep trench filling.

2
Experiments and discussion

The samples for the trench filling were prepared by deep reactive ion etching (DRIE) the Si substrate using a negative-resist mask. The trenches were etched by SF_6 and O_2 ICP plasma (STS Co.). The etched trenches were all about 50–75 μm deep with widths varying from 4 to 50 μm. All the CVD was done in the deposition reactor illustrated in Fig. 2. The organic source, TEOS of ultrahigh purity (99.99%) (Yamanaka Hutech Chemicals Co.), was evaporated directly by a vaporizer and delivered into a heated gas pipe kept at 90 °C to avoid liquefaction of TEOS. The ozonizer generated O_3 from pure O_2 by the silent discharge at atmospheric pressure. TEOS vapor and O_3/O_2 were mixed near the region of the dispersion head and formed a downstream flow above the substrate. The other kinds of gas, Ar or C_2F_6, were piped into the chamber and injected above the substrate. The deposition reactor assembly was composed of a dispersion head (or a coil antenna), a heated stage, and a cold wall chamber. The dispersion head can be exchanged with a coil antenna. The RF power was delivered into the dispersion head through a matching box. The stage was grounded and the RF powers are all of 13.56 MHz unless otherwise noted. The chamber was evacuated down to 1 mTorr by rotary and mechanical booster pump before deposition. The pressure of the chamber was controlled by tuning the main valve manually.

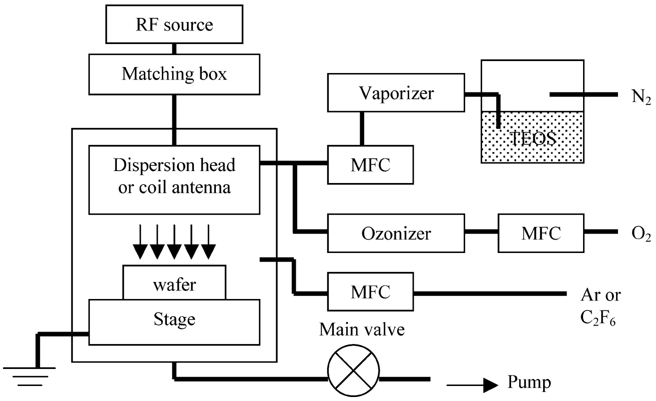

Fig. 2. Schematic diagram of the deposition reactor

After every deposition, the film was characterized by measuring the thickness and the refractive index (Nanospec film thickness system). The conformality was estimated by scanning electron microscope (SEM). The film stress was calculated using the Stoney equation [20] where the curvature radius of the substrate was measured with a surface profiler (KLA/Tencor).

3.1
PECVD oxide 1: ICP oxide

An immersed coil antenna was used to excite ICP producing high density plasma [19] as shown in Fig. 3. O_3/O_2 mixture, and Ar were injected into the top of the coil, and TEOS vapor was injected between the coil and the stage [21]. Here the typical deposition conditions were listed as follows: O_2 (7.3% O_3): 5 sccm, TEOS: 1 sccm, Ar partial pressure: 26 mtorr, temperature: 350 °C, total pressure: 45 mtorr, coil RF power density: 0.25 W/cm_2. The deposition rate was about 78 Å/min, the refractive index of the oxide was 1.38, and the film stress was about 95 MPa tension.

Here only a small amount of Ar was introduced to sputter the wafer to enhance the gap filling capability of the CVD [9–11]. During the deposition, at the same time, the high density ion bombardment of the substrate with high energy provides a sputtering effect such that the deposition profile can be modified to reduce the void formation, and simultaneously a good quality oxide can be deposited at a high deposition rate.

Figure 4a shows the PECVD oxide deposited by the coil antenna ICP with Ar supplied. The sidewall step coverage, c/a, is much lower than the bottom step coverage, b/a, because the ion species basically contribute the most to the vertical deposition component due to their directionality to the substrate. If Ar is not introduced into reaction, the oxide overhangs will occur on the trench edge as shown in Fig. 4b under the same conditions. It is attributed to that the charges accumulate on the trench edge and attract ion species, so that the deposition rate on the trench edge is higher than other surface region.

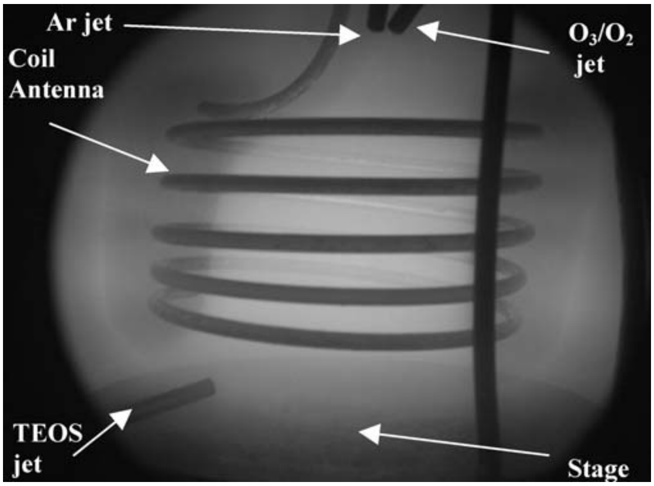

Fig. 3. Coil-antenna ICP

Comparing Fig. 4a with b, the trench edge was etched by this in-situ Ar ion sputtering [10, 11, 22], but not very significantly. Even though several studies relating deposition and sputter etch cycles aiming at trenches filling have been studied, the deeper the trenches are, more time and cycles are required. It was very difficult and time-consuming to fill the trenches of high aspect ratio (>10) by using deposition and sputter etch cycles [9, 11].

On the contrary, enhancing Ar ion sputtering the PECVD oxide increases the possibilities of sealing trench-etched structures. Under the same conditions Fig. 4c shows the oxide deposited by the coil antenna ICP under the stage RF power density 1.25 W/cm$_2$ applied. The trench openings were closed off and sealed as closed micro-channels under the irradiation of enhanced high density plasma. The effect of Ar ion sputtering was further enhanced as the stage RF power increased. Simultaneously the stage DC bias was increased, and resulted in the ions acceleration. Since ions are energetic species compared to the neutral species, the surface mobility may play only a minimal role during SiO_2 deposition [9, 10, 22]. It is the main reason that PECVD oxide deposited by coil antenna ICP generates a shoulder on a trench edge faster and seals a trench easier than the other deposition methods. Because the surface mobility of the oxide precursor was kept to a minimum, the sidewall step coverage was also reduced to a minimum as shown in Fig. 4c [9].

3.2
PECVD oxide 2: CCP oxide

The capacitive coupled plasma (CCP) was excited between the parallel electrode plates as shown in Fig. 5. The stage was the lower electrode plate, and the dispersion head was the upper electrode plate. Here the typical deposition conditions were listed as follows: O_2 (7.6% O_3): 130 sccm, TEOS: 12 sccm, temperature: 350 °C, total pressure: 90 mtorr, RF power density: 2.5 W/cm$_2$, electrode gap: 14 mm. The deposition rate was about 700 Å/min, the refractive index of the oxide was 1.462, and the film stress was about 159 MPa tension.

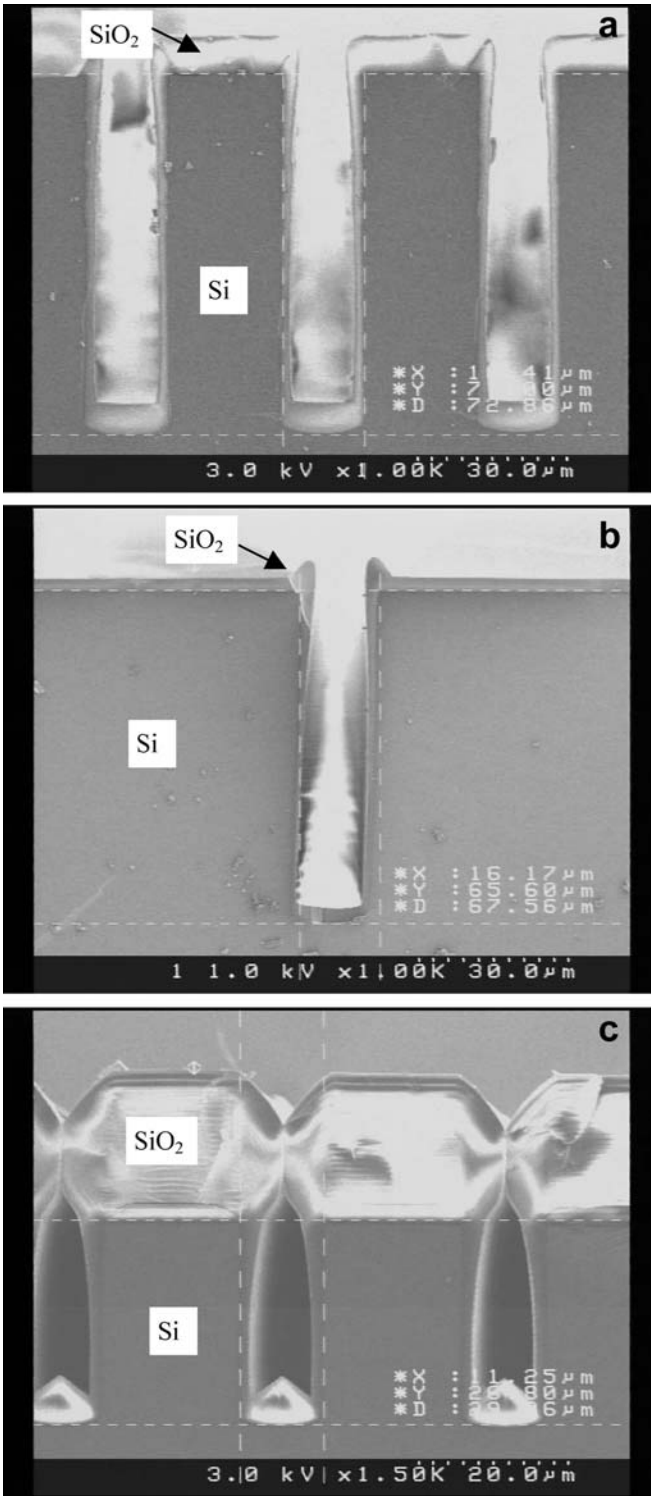

Fig. 4. **a** Oxide deposited by coil antenna ICP with Ar supplied, **b** oxide deposited by coil antenna ICP without Ar supplied, **c** trenches closed off by the coil antenna ICP oxide under the stage RF power applied

Figure 6a shows the PECVD oxide deposited by the parallel plates capacitive coupled plasma (CCP). The sidewall step coverage, c/a, is also lower than the bottom step coverage, b/a, because of the ion directionality of CCP oxide similar to that of ICP oxide. However, the trench

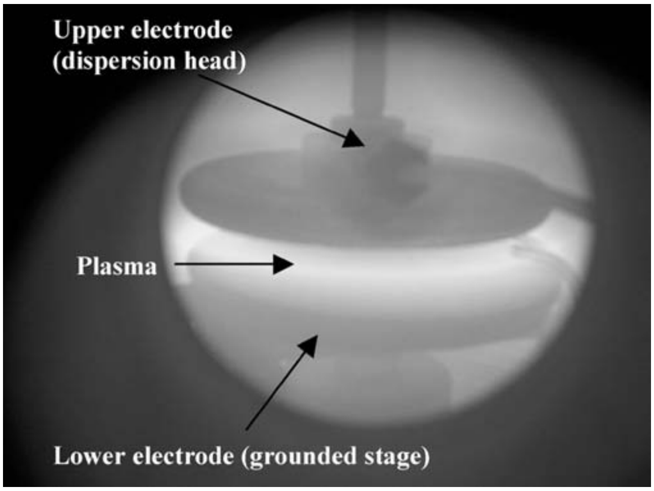

Fig. 5. Parallel plates CCP

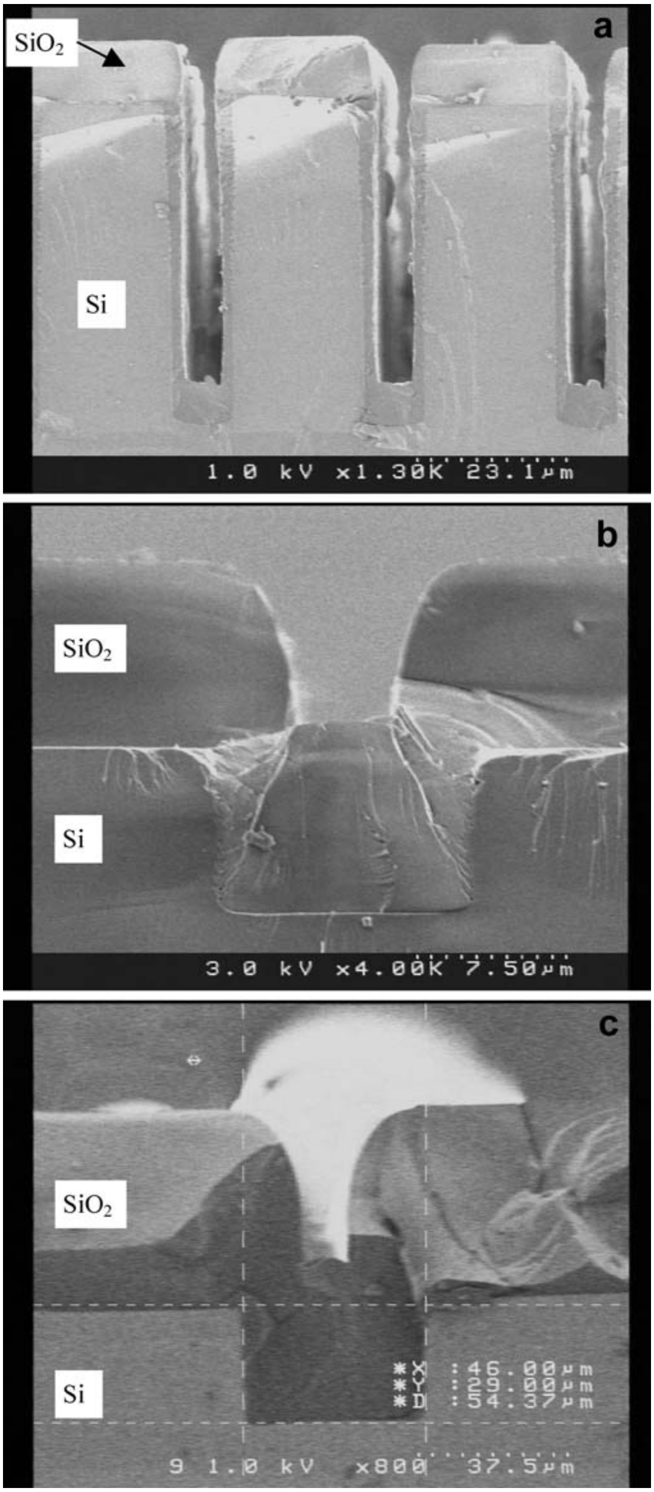

Fig. 6. **a** Oxide deposited by parallel plates CCP, **b** trench filled by the parallel plates CCP oxide, **c** trench filled by the parallel plates CCP oxide under the magnetic field applied

filling capability of the CCP oxide is better than that of ICP oxide. Figure 6b shows the trench filled by this CCP oxide.

To increase the plasma density, magnets of 1.7 kGauss were added beneath the stage. The deposition rate of the plasma enhanced by this magnetic field was much increased up to five times of that without the magnetic field. Figure 6c shows the trench filled by the oxide of CCP enhanced by this magnetic field. Even though the step coverage is not conformal, this thick and impermeable SiO$_2$ filled in shallow trenches is suitable for applications that need to maintain large pressure difference between the two sides of the layers, contain fluid within layers, isolate any heated MEMS devices, or suspend high temperature power MEMS devices [3, 8].

3.3
SACVD oxide

The deposition reactor of SACVD is the same to that of CCP PECVD, but no RF power applied. Here the typical deposition conditions were listed as follows: O$_2$ (7.6% O$_3$): 42 sccm, TEOS: 4 sccm, temperature: 375 °C, total pressure: 22.5 torr, electrode gap: 6 mm. The deposition rate was about 161 Å/min, the refractive index of the oxide was 1.461, and the film stress was about 85 MPa compression.

The oxide deposition of SACVD yields excellent step coverage as shown in Fig. 7a, because the only neutral radials were generated during CVD reaction. Very high conformality was achieved for 375 °C and 22.5 torr deposition into a deep trench of 60.3 μm depth, 9.4 μm width, and aspect ratio was 6.4. The trenches of 52 μm depth and 5 μm width (aspect ratio = 10.4) were completely filled as shown in Fig. 7b. It is attributed to that the intermediate precursor of SiO$_2$ possesses high surface mobility during CVD reaction due to the high O$_3$ concentration (7.6%) and the high flow rate ratio of O$_3$ to TEOS (10.5) [16–18, 23]. The step coverage varies with the aspect ratio of the trench as shown in Fig. 8. The etched trenches were all about 50–75 μm deep with widths varying from 4 to 50 μm. In Fig. 8a, the bottom step coverages have no obvious differences between three types of SiO$_2$ under the low aspect ratio (<4) of trenches, but SACVD oxide provides higher bottom step coverage than others as the aspect ratio of the trenches larger than 5. It is attributed to that the overhang formation on the trench edge reduces the possibilities of the gas phase intermediate of PECVD oxide falling down to the trench bottom. In

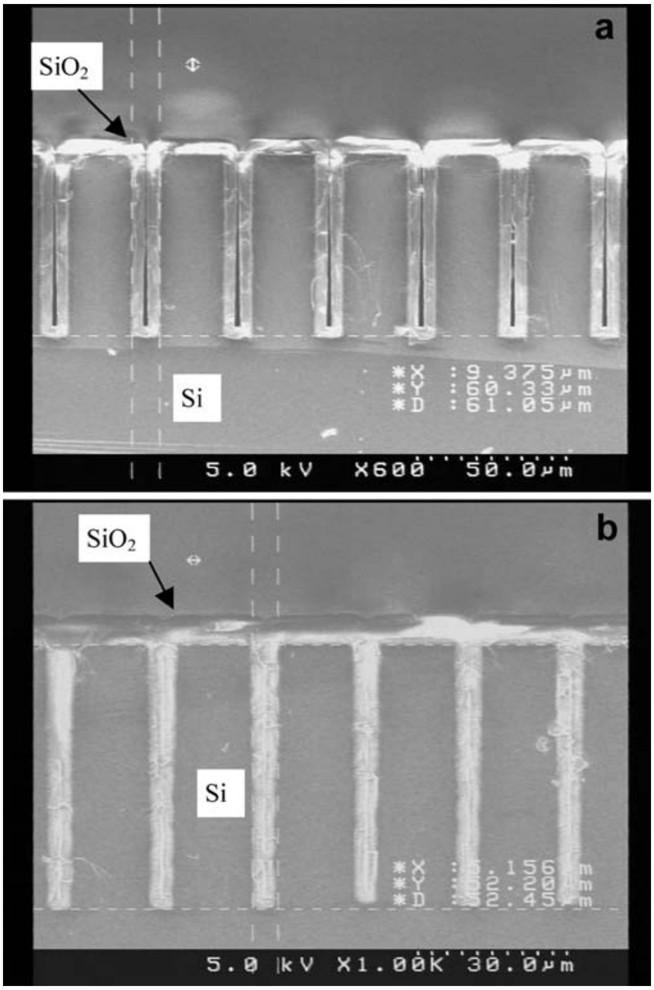

Fig. 7. **a** High conformality of SACVD oxide, **b** trench filling and planarization of the SACVD oxide

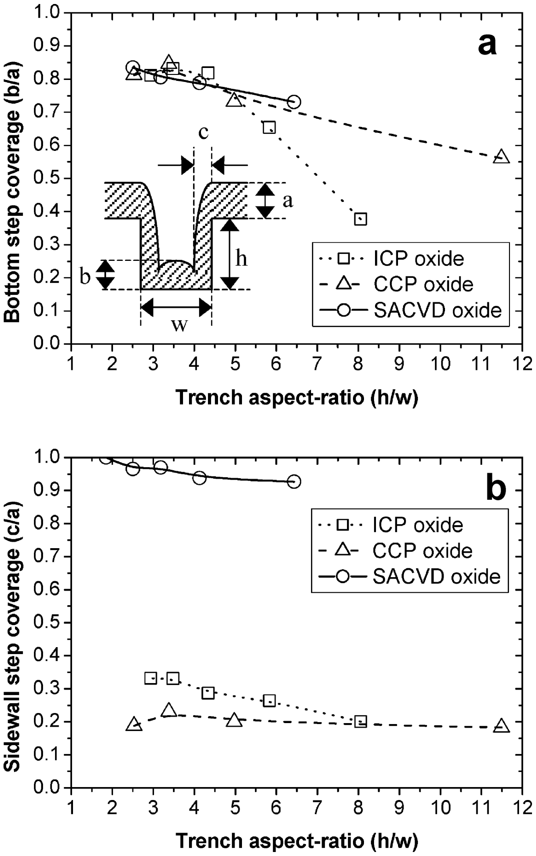

Fig. 8. **a** Bottom step coverage varying with trench aspect ratio, **b** sidewall step coverage varying with trench aspect ratio

Fig. 8b, the sidewall step coverage of SACVD is much better than those of the other two PECVD oxides, and keeps larger than 92% as the aspect ratio of the trench up to 6.5 and even approaches 100% as the aspect ratio down to 1.85. Comparing Fig. 8a with b, it should be noted for SACVD oxide that the bottom step coverage is lower than the sidewall step coverage, because of the surface diffusion of the intermediate precursor during SACVD reaction. Besides, it also should be noted for CCP and ICP oxides that the sidewall step coverages are lower than the bottom step coverages, because of the ion directionality to the substrate during PECVD reaction.

4
Conclusion

The TEOS/ozone SiO2 films deposited by PECVD and SACVD for trench filling were characterized in this paper. Two types of PECVD were utilized: Coil antenna inductively coupled plasma (ICP) and parallel plates capacitive coupled plasma (CCP). Coil antenna ICP produces oxide films with higher deposition rate than others, but results in poor step coverage, even though in-situ Ar ion sputtering can impede the overhang formation on the trench edge. In general, for the same trench width, trenches can be closed from the trench top by a thick PECVD layers, especially an ICP oxide layer. This is a good candidate for trench sealing application.

The oxide film deposited by parallel plates CCP has similar step coverages to that deposited by coil antenna ICP. The CCP enhanced by the magnetic field can increase deposition rate drastically. Even though the step coverage is non-conformal, this CCP is suitable for producing a thick and impermeable SiO_2 layer filled in shallow trenches for applications that need to maintain large pressure difference between the two sides of the layers, contain fluid within layers, or isolate any heated MEMS devices.

The step coverage for SACVD oxide is much better than those of the other two PECVD oxides. Step coverage in high aspect-ratio trenches improves significantly by utilizing SACVD process. The complete planarization and deep trench filling have been achieved successfully by utilizing SACVD. Very high conformality was achieved for 375 °C deposition into a deep trench (60.3 µm depth and 9.4 µm width, aspect ratio = 6.4) and essentially 100% conformality (52 µm depth and 5 µm width, aspect-ratio = 10.4) was obtained. Low temperature (<400 °C) SACVD deposition resulted in the low residual stress about 85 MPa compression. We conclude that the SACVD TEOS/ozone process is capable of depositing low stress films with excellent step coverage at low temperature. Further more detailed experiments have been conducted to characterize SACVD oxide to fill the trenches of higher aspect ratio recently. In the future the SiO_2 film capable of filling deep trenches will be surely and widely applied in microsystems.

References

1. **Homma T** (1998) Low dielectric constant materials and methods for interlayer dielectric films in ultralarge-scale integrated circuit multilevel interconnections. Mater Sci Eng R23: 243–285
2. **Ayazi F; Najafi K** (2000) High aspect-ratio combined poly and single-crystal silicon (HARPSS) MEMS technology. J MEMS 9(3): 288–294
3. **Zhang C; Najafi K** (2002) Fabrication of thick silicon dioxide layers using DRIE, oxidation, and trench refill. MEMS2002, Las Vegas, US, pp. 160–163
4. **McCann P; Somasundram K; Byrne S; Nevin A** (2001) Conformal deposition of LPCVD TEOS. In: Proc SPIE, Micromachining & Microfabrication Process Technology VII 4557: 329–340
5. **Rusu C; Klaasse G; Sedky S; Esch H; Parmentier B; Verbist A; Witvrouw A** (2001) Planarization of deep trenches. In: Proc SPIE, Micromachining & Microfabrication Process Technology VII 4557: 49–57
6. **Zhang D; Li Z; Li T; Wu G** (2001) A novel isolation technology in bulk micromachining using deep reactive ion etching and a polysilicon refill. J Micromech Microeng 11: 13–19
7. **Parviz BA; Najafi K** (2001) A geometric etch-stop technology for bulk micromachining. J Micromech Microeng 11: 277–282
8. **Arana LR; Schaevitz SB; Franz AJ; Jansen KF; Schmidt MA** (2002) A microfabricated suspended-tube chemical reactor for fuel processing. MEMS2002, Las Vegas, US, pp. 232–235
9. **Pai CS** (1996) High quality voilds free oxide deposition. Mater Chem Phys 44: 1–8
10. **Den Boer DJ; Fukuda H; Helmig J; Van Der Hilst JBC; Janssen GCAM; Kalkman AJ; Radelaar S** (1998) SiOF and SiO_2 deposition in HDP reactor: tool characterization and film analysis. Microelectron Reliab 38(2): 281–286
11. **Schwartz GC; Johns P** (1992) Gap-fill with PECVD SiO_2 using deposition/sputter etch cycles. J Electrochem Soc 139(3): 927–932
12. **Shareef IA; Rubloff GW; Anderle M; Gill WN; Cotte J; Kim DH** (1995) Subatmospheric chemical vapor deposition ozone/TEOS process for SiO_2 trench filling. J Vac Sci Technol B 13(4): 1888–1892
13. **Xia LQ; Conti R; Galiano M; Campana F; Chandran S; Cote D; Restaino D; Yieh** E (1999) High aspect ratio trench filling using two-step subatmospheric chemical vapor deposited borophosphosilicate glass for <0.18 μm device application. J Electrochem Soc 146(5): 1884–1888
14. **Huang J; Kwok K; Witty D; Donohoe K** (1993) Dependence of film properties of subatmospheric pressure chemical vapor deposited oxide on ozone-to-tetraethylorthosilicate ratio. J Electrochem Soc 140(6): 1682–1686
15. **Xia LQ; Yieh E; Gee P; Campana F; Nguyen BC** (1997) Process characteristics for subatmospheric chemical vapor deposited borophophosilicate glass and effect of carrier gas. J Electrochem Soc 144(9): 3208–3212
16. **Matsuura M; Hayashide Y; Kotani H; Abe H** (1991) Film characteristics of APCVD oxide using organic silicon and ozone. Jpn J Appl Phys 30(7): 1530–1538
17. **Ikeda Y; Numasawa Y; Sakamoto M** (1990) Ozone/organic-source APCVD for conformal doped oxide films. J Electronic Mater 19(1): 45–49
18. **Fujino K; Nisimoto Y; Tokumasu N; Maeda K** (1990) Silicon dioxide deposition by atmospheric pressure and low-temperature CVD using TEOS and ozone. J Electrochem Soc 137(9): 2883–2887
19. **Sugai H; Nakamura K; Suzuki K** (1994) Electrostatic Coupling of antenna and the shielding effect in inductive RF plasmas. Jpn J Appl Phys 33(1)4B: 2189–2193
20. **Chang S; Eaton W; Fulmer J; Gonzalez C; Underwood B; Wong J; Smith RL** (1991) Micromechanical structures in amorphous silicon. International Conference on Solid-State Sensors and Actuators 751–754
21. **Hitchman ML; Alexandrov SE** (2001) New approaches to Titania and Silica CVD. The Electrochem Soc Interface, Summer 2001, pp. 40–45
22. **Gross M; Horwitz CM** (1993) Silicon dioxide trench filling process in a radio-frequency hollow cathode reactor. J Vac Sci Technol B 11(2): 242–248
23. **Adachi M; Okuyama K; Fujimoto T; Sato J; Muroyama M** (1996) Morphology control of films formed by atmospheric-pressure chemical vapor deposition using tetraethylorthosilicate/ozone system. Jpn J Appl Phys 35(1) 8: 4438–4443